Energy Conversion and Management: X 24 (2024) 100793

Contents lists available at ScienceDirect

Energy Conversion and Management: X

journal homepage: www.sciencedirect.com/journal/energy-conversion-and-management-x

Hybrid renewable energy systems for sustainable power supply in remote location: Techno-economic and environmental assessment

Dibyendu Roy [a,*], Ruiqi Wang [a,*], Sumit Roy [a,b], Andrew Smallbone [a], Anthony Paul Roskilly [a]

[a] *Department of Engineering, Durham University, Durham DH1 3LE, UK*
[b] *Centre for E-Mobility and Clean Growth, Coventry University, Coventry CV1 2TL, UK*

ARTICLE INFO

Keywords:
Techno-economic analysis
Levelised cost of energy
Hybrid renewable energy systems
Life cycle assessment
Hydrogen

ABSTRACT

Electricity supply is inconsistent and unreliable in many remote areas of India, where depending solely on a single renewable energy source is impractical. In this context, this study investigates the potential of off-grid hybrid renewable energy systems (HRES) to meet the energy needs of a village community in India. Techno-economic analysis and life cycle assessment have been employed to compare eleven HRES combinations which combine photovoltaic (PV), wind turbine (WT), battery (BAT), diesel generator (DG), biogas generator (BG), converter (CONV), and electrolyser (ELEC). By optimising the size and capacity of each component in HRES, this study aims to identify the combination with the lowest levelised cost of energy (LCOE). This research aligns with United Nations Sustainable Development Goal No. 7 to seek “Affordable and Clean Energy”. The findings highlight that HRES comprising PV/WT/BAT/CONV/DG exhibits the lowest LCOE (0.319 $/kWh) and net present cost (6.81 M$) among all combinations. In systems with partial reliance on diesel, integrating both PV and WT could reduce diesel consumption and increase the renewable fraction to 86.7 %. For HRES involving PV, a significant contribution to greenhouse gas emissions occurs during the construction stage. The WT/DG combination, with its high diesel dependency, has the largest global warming potential. The efforts from this study provide valuable insights into determining the optimal HRES for remote communities by considering their economic and environmental factors.

1. Introduction

1.1. Background and motivation of the study

The renewable energy capacity of India as of December 2021 stands at 104.88 GW, with an additional 56.31 GW currently being implemented [1]. In line with the COP 26 declaration, the Indian government has set its sights on establishing a 500 GW non-fossil energy capability by 2030, as it endeavours to realise its target of attaining net-zero emissions by 2070 [1]. To reach this net zero goal, it will require significant effort and policy related changes by the government of India. Nearly 70 % of the population of India resides in rural regions, where most of the people still depend on kerosene, diesel and solid biomass to meet their energy requirements. In this regard, several government schemes such as the Roof Top Solar (RTS) Programme, and the Deendayal Upadhyaya Gram Jyoti Yojana (DDUGJY) [2] have been implemented by the Indian government to provide the renewable electricity. Although many rural and remote locations of India have been electrified, several parts of India still face frequent power outages [3]. In this context, hybridisation of energy system which integrates two or more renewable energy sources with non-renewable sources such as diesel generators, could be a viable solution for rural and remote areas.

The Sundarbans, which is renowned for its mangrove forest, is a collection of shallow islands located in the Bay of Bengal and stretches across India and Bangladesh [4]. Establishing traditional grids may not be a good option for the isolated islands of Sundarbans due to the difficult terrain and maintenance-related challenges. Furthermore, the high intensity cyclones that occur frequently [5] in the region intensify the risks to traditional power grids. On the other hand, the adoption of intelligent microgrids could result in decreased operational expenses, diminished emissions, enhanced energy efficiency, and increased system reliability [6]. Previously attempts have been taken by governments to install photovoltaic (PV) based system to supply required electricity to some villages located at the Sundarbans area [7]. It is important to note that Sundarbans is rich in forestry biomass, thus biomass-based energy systems can also be implemented. Nevertheless, smart microgrids with adaptable energy storage systems that incorporate a variety of

* Corresponding authors.
E-mail addresses: dibyendu.roy@durham.ac.uk (D. Roy), ruiqi.wang@durham.ac.uk (R. Wang).

https://doi.org/10.1016/j.ecmx.2024.100793
Received 19 September 2024; Received in revised form 8 November 2024; Accepted 9 November 2024
Available online 10 November 2024

Nomenclature

Abbreviations

BAT	Batteries
BG	Biogas generators
CAP	Capital cost
CONV	Converters
CRF	Capital recovery factor
DG	Diesel generator
ELEC	Electrolyser
FC	Fuel cell
GHG	Greenhouse gas
HRES	Hybrid renewable energy systems
LCA	Life cycle assessment
LCIA	Life cycle impact analysis
LCOE	Levelised cost of energy
MCDM	Multi-criteria decision making
NPC	Net present cost
O&M	Operating and maintenance
PEM	Polymer electrolyte membrane
PV	Photovoltaic
RC	Replacement cost
ROI	Return on investment
RTS	Roof top solar
SDG	Sustainable Development Goal
SL	Salvage cost
TK	Tank
WT	Wind turbines

Symbols

C_{annual}	Total annual cost, $
$Capacity_A$	Capacities of the reference components, kW
$Capacity_B$	Capacities of the built components, kW
d_n	Real discount rate, %
E_{GEN}	Total annual electricity generation, kWh/yr
E_{PV}	Energy generated from the PV arrays, kW
f	Scale factor
f_r	Rate of inflation
FD_{PV}	Derating factor of PV
$\overline{I_T}$	Incident solar irradiance on the PV array, kWh/m^2/day
$\bar{I}_{T,STC}$	Irradiance incident at the STC, kWh/m^2/day
In_A	Input materials and energy for the reference components
In_B	Input materials and energy for the built components
LHV_{fuel}	Lower heating value of the fuel, kJ/kg
m_{fuel}	Mass flow rate of fuel, kg/s
N_k	The number of components
N_{PV}	Number of PV arrays
P_{BG}	Power output of the generator, kW
$T_{a,NOCT}$	Ambient temperature, K
T_C	Temperature of the PV cell, K
$T_{C,NOCT}$	Operating (nominal) cell temperature, K
$T_{C,STC}$	temperature of the cell under STC, K
T_k	Lifetime of component, year
$T_{k,rem}$	Remaining lifespan of the kth component, year
$T_{Pro,j}$	Lifetime of the project, year
V	Velocity, m/s
$V_{cut,in}$	Cut-in wind speed, m/s
$V_{cut,off}$	Cut-off wind speed, m/s
V_{rated}	Rated wind velocity, m/s
W_{PV}	Power output of a photovoltaic array, kW
$\dot{W}_{rated}$	Rated power, kW
W_{WT}	Power delivered by the wind turbines, kW
Z_{PV}	Rated capacity of PV array, kW
Δt	Time-period, hour

Greek letters

β_t	Temperature coefficient of power
η_{BG}	Electrical efficiency of the BG
$\eta_{MP,STC}$	Maximum power efficiency achieved under STC

Subscripts

k	the k^{th} component

renewable energy sources like solar, wind, biomass, etc., could provide an alternate solution for meeting the energy demands of local communities.

1.2. Literature review

To achieve the energy security and environmental sustainability goals, hybrid renewable energy system (HRES) has shown great potential across multiple applications, such as the transportation systems [8], the industrial sectors [9], and residential communities [10], etc. The HRES also plays a critical role in facilitating the shift from fossil fuels to renewable energy [11]. Due to the intermittent nature of renewable energy system, combining various renewable resources within a hybrid system could better meet the varying electricity demands throughout the day [12]. Optimal combination is normally identified through optimisation methodology applied among various HRES scenarios, considering factors including the component size, generation types, and energy storage pathways [13]. Numerous research studies have been carried out globally in the field of optimal HRES tailored to specific areas. Kumar and Channi [14] used the TOPSIS method to optimise a PV-biomass energy system with battery (BAT) storage for a rural village and reported that the optimal HRES has total generation of 3650 kWh per year, with PV and biomass generator contributing 35.6 % and 64.4 % to renewable electricity, respectively. Mulumba and Farzaneh [15] conducted a multi-objective optimisation for a hybrid PV-wind turbine (WT)-BAT-flywheel system for off-grid power supply in a remote area in Kenya, concluding that an optimised size of HRES with 26 PV panels (330 W) and 3 WTs (1 kW) could meet the local demand requirement of 37.94 MWh. In Pakistan, He et al. [16] investigated a WT-PV-BAT-DG based HRES in a remote area using hierarchical optimisation methods, and demonstrated that subsidy policies could increase renewable energy utilisation to 99.23 % and reduce lifecycle carbon emissions by 80.7. By using the decision-making variables such as the type and number of WT, number of storage units, capacity of solar panels and biogas generator, Sadeghi et al. [10] designed an optimised HRES combining BG/PV/WT/BAT/ converter (CONV) for a village in Iran. The optimal setup, including a 22 kW BG, 30.7 kW PV, 10 kW WT, 11 BAT, and a 15.1 kW CONV, yielded an energy cost of 0.201 $/kWh. These studies underscore the importance of accurately matching power supply and demands when optimising the HRES, but the practical acceptance of HRES will further depend on their economic feasibility.

Economic analyses of HRES frequently assess indicators including cost of electricity, net present cost (NPC), and profitability of investment, which have been explored in various studies to guide economic feasibility assessment. For example, El-houari et al. [17] investigated an optimum HRES for an isolated rural Moroccan village based on the most cost-effective option of which the initial investment cost of $49,524.4, maintenance cost of $4,008, a NPC of $123,887, and a cost of electricity of 0.2 $/kWh could be achieved. Previously, Roy [18] used machine learning for optimising an off-grid HRES in a remote area, reporting a minimum LCOE of 0.31 $/kWh, and the maximum return on investment (ROI) of 26.4 %. A techno-economic analysis of HRES configuration

Table 1
Summary of related studies of environmental assessment on optimised HRES.

Ref.	HRES components	Scope	Function unit	Impacts categories	Key findings
[28]	PV, WT, DG, BAT	Raw material processing and assembly, installation, operation, end-of life stages of system	Generation and supply of 1 kWh of electricity	Midpoint ReCiPe impacts indicators	The system with PV, WT, and lead acid BAT has the lowest impacts and enhances the reliability of renewable power
[29]	PV, WT, solar collector, heat pump, BAT	Production and transport of parts, operation, and maintenance of the system	Generation of 1 kWh electricity	Environmental footprint	Solar PV can reduce most environmental impacts in grid-connected system
[30]	PV, WT	Installation and operation stages	Generation of 1 kWh electricity	Annualised embodied carbon and carbon footprint	Stand-alone HRES can reduce annual GHG emissions ranging 5.4–6.6 million kg of CO_2 equivalent compared to grid power
[31]	PV, WT, biomass engine	Construction and production stages	Supply of 1 kWh electricity	Life-cycle CO_2 emissions	5 % of increase in investment of magnitude leads 50 % reduction in emissions
[32]	PV, WT, BAT	Production, distribution, transportation, operation of energy components	Producing 1 m^3 freshwater	IMPACT 2002 + method indicators	Building and operating PV system have more damage to the environment and human health than a wind farm
[33]	PV, WT, biogas generator (BG), ELEC, BAT	Operation stage	Supply electricity in one year	CO_2, CO, and NO_X emissions	Combination of ELEC with PV, WT, and BG has the highest CO_2 emissions
[34]	PV, WT, natural gas combined cycle	Embodied water and energy in the raw materials, process energies, and the end-of-life energy	Withdrawal of water throughout one year	Direct and indirect carbon emissions	Scenario of HRES has the highest economic cost and lowest environmental cost of products, revealing the need of support from governmental subsides
[35]	WT, DG, ELEC, FC	Manufacturing, transportation, operation, and maintenance stages	Supply of electricity over 20 years	CO_2 emissions	The HRES has potential to reduce CO_2 emissions by 70,529t over its lifespan, with a carbon reduction cost of 38 \$/t CO_2

integrating PV/BAT/WT/CONV with grid for a coastal region in Bangladesh proved that the system can yield LCOE of 0.03$/kWh and generate 4,604.591 MWh of electricity annually [19]. Furthermore, Das et al. [20] expanded the combination of HRES with fuel cell (FC) and electrolyser (ELEC) for a remote village in Sundarban and investigated this configuration by employing technoeconomic, multi criteria decision making (MCDM), and Monte Carlo based risk analysis, which showed that an optimal LCOE of $0.159/kWh, a net present cost of $424,568, and a renewable fraction of 96.5 % could be achieved. Another study by Das et al. [21] examined five energy storage devices (lead-acid, lithium-ion, vanadium redox, zinc-bromide batteries, and pumped hydro energy storage) incorporated in HRES using two dispatch strategies (load following and cycle charging) for a remote village, achieving an optimal solution with LCOE of 0.197 $/kWh, NPC of $362,384, and renewable fraction of 89.17 %. Singh and Rizwan [12] explored an off-grid PV/BG/BAT/CONV system to fulfill the load requirements in a rural community in India, in which an optimal configuration with a net present cost of $57,283 and LCOE of $0.61/kWh was identified. These studies evaluated technical and economic performance of HRES through comparative evaluation of economic indicators, providing prerequisite to supply sustainable power in remote areas. However, these studies did not account for the embodied energy, resources consumption, and environmental impacts throughout the entire life cycle of HRES, leading to an incomplete assessment from environmental aspects.

To address this, life cycle assessment (LCA) is essential, as it evaluates environmental implications at each stage of the systems' life cycle, which supports decision making for sustainable energy systems [22]. The studies regarding LCA on HRES have been carried out on the integration of various renewable technologies and their environmental impact assessments across different geographical locations. For instance, Khan et al. [23] studied the LCA of a WT and FC integrated energy system, reporting a life cycle GWP of 40.6 CO_2 equivalent/kWh. Similar LCA related studies on energy systems were reported by Lai and Adamas [24], Rillo et al. [25], and Jolaoso et al. [26]. But these studies did not conduct a comprehensive LCA based on the optimal size of each component in the HRES. For the optimal designed HRES, Das and De [3] conducted a study on a HRES consisting of DG, PV, WT, CONV, and BAT to cater to the energy demand of a remote village in India. The study presented a techno-economic and environmental assessment upon a feasible optimum solution resulting from MCDM approach, reporting that an environmental impact lesser than 40.5–82 % of HRES could be achieved. Similarly, Nagapurkar and Smith [27] examined an optimised microgrid by using genetic algorithm in three US cities with techno-economic analysis and greenhouse gas (GHG) emissions estimation, which reported low carbon footprint and LOCEs ranged from 0.32-0.42 $/kWh. More studies on environmental assessment of optimised HRES are summarised in Table 1. It can be found that most studies focus on the carbon emissions during the construction and operation stages of HRES, while a few studies applied LCA to consider broader impact categories such as human health and ecosystems across all life stages of HRES. By considering the local availability of renewable energies, further combinations of HRES could be explored and evaluated by using LCA for a more comprehensive environmental analysis.

1.3. Novelty and contribution of the study

In the remote regions of India, where a substantial portion of the population resides, often encountered difficulties related to the inconsistent and unreliable supply of electricity. Depending solely on a single renewable energy source for providing electricity may not represent a practical solution due to the inherent uncertainties and difficulties involved. The uncertainty associated with an energy system with a single renewable energy source can be avoided by the implementation of a smart HRES configuration, as it enables the integration of multiple renewable sources, offering a more resilient energy solution. Meanwhile, the implementation of energy storage facilities, such as batteries and electrolysers for green hydrogen production could improve the stability of renewable power outputs.

The literature reviews indicate previously various research investigated simulation-based studies on HRES integrating combining renewable as well as partial non-renewable sources using techno-economic [36–38] and various optimisation strategies [39–41]. However, these studies overlooked diverse combinations that consider local renewable energy availability. Additionally, there is a lack of studies using LCA to evaluate the environmental performance of optimised HRES, including systems with biomass generator and hydrogen electrolyser throughout their entire lifespan.

To fill this research gap, this study aims to investigate various off-grid HRES combinations based on different considerations of renewable energy to meet the energy demands of a community on Satjelia village in the Sundarbans, West Bengal, India. The components in each combination are optimised for size and capacity to achieve the minimum LCOE. The objective of this study is consistent with United Nations Sustainable Development Goal (SDG) No. 7, which seeks to provide

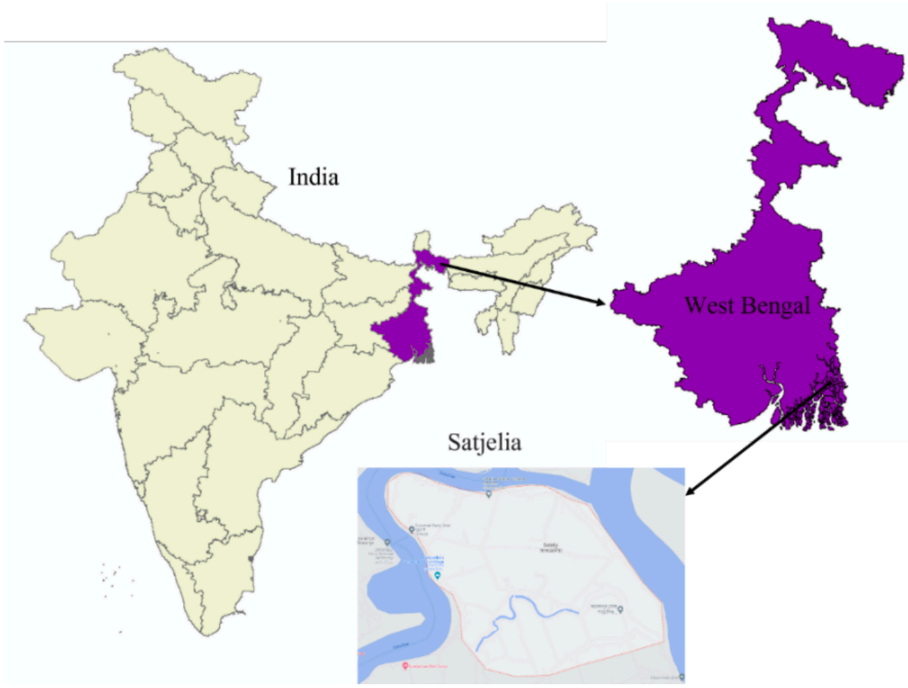

Fig. 1. Location of the study.

"Affordable and Clean Energy"[42]. By considering local availability of renewable energy resources, a comprehensive techno-economic analysis as well as environmental impacts assessment are conducted for eleven HRES combinations that include PV, WT, BAT, DG, BG, CONV, and ELEC components, to offer a sustainable energy solution for the remote community. This study makes contributions in several aspects:

- It investigates the feasibility of eleven HRES combinations as alternatives to traditional fossil fuel-based electricity generation in the Satjelia village community. By considering local renewable resources availability and energy prices, the optimisation of each combination is conducted with respect to component size and capacity to obtain the optimised system design.
- The techno-economic analyses for all HRES combinations compare key economic indicators such as the LCOE and NPC. The evaluation of different cost items provides insights into the economic benefits of using various renewable energy sources within the HRES, therefore offering a reference for selecting the most suitable combination for the local area.
- A detailed environmental impacts assessment is performed through LCA using SimaPro software with the ReCiPe 2016 midpoint method for all eleven HRES combinations. It explores the environmental

Table 2
Energy demand of the location.

Load category	Appliances	Quantity	Watt	Summer (Mar-Oct)		Winter (Nov-Feb)	
				Usage (hr)	Load (Wh/d)	Usage (hr)	Load (Wh/d)
Demand of one house	Lighting	3	40	7	840	7	840
	Fan	2	70	8	1,120	0	0
	Television	1	100	5	500	5	500
	Mobile charger	1	10	1	10	1	10
	Miscellaneous	1	100	1	100	1	100
Number of houses					2,200		2,200
Total demand (kWh/d)					5,654		3,190
Demand of one primary school	Lighting	15	40	8	4,500	8	4,800
	Fan	10	70	8	5,600	8	5,600
	Water pump	1	746	1	746	1	746
	Computer	1	100	8	800	8	800
Number of schools					2		2
Total demand (kWh/d)					23.892		23.892
High school	Lighting	50	40	8	16,000	8	16,000
	Fan	40	70	8	22,400	8	22,400
	Water pump	1	746	1	746	1	746
	Computer	5	100	8	4,000	8	4,000
Total demand in high school (kWh/d)					43.146		43.146
Primary health centre	Lighting	30	40	12	14,400	12	14,400
	Fan	40	70	12	1,6800	0	0
	Water pump	1	746	2	1,492	2	1,492
	Computer	3	100	12	3,600	12	3,600
	Refrigerator	2	150	24	7,200	24	7,200
Total demand in primary health centre (kWh/d)					43.492		26.692
Total demand of the location (kWh/d)					5,764.53		3,283.73

Table 3
Monthly wind speed at the location.

Month	Jan	Feb	Mar	Apr	May	Jun	July	Aug	Sep	Oct	Nov	Dec
Wind speed (m/s)	4.01	3.97	4.61	5.63	5.68	6.23	6.24	5.48	4.61	3.43	3.53	3.93

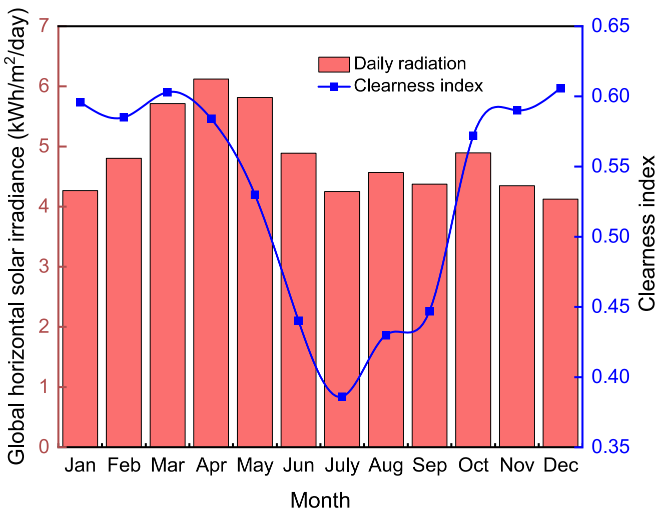

Fig. 2. Solar irradiance and clearness index at the study location.

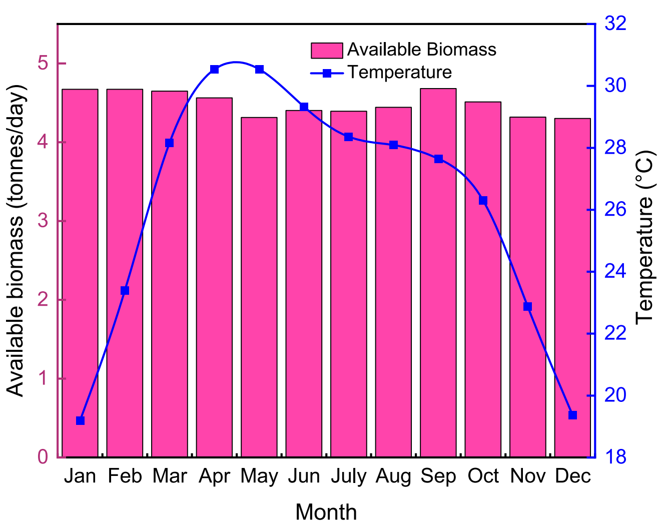

Fig. 3. Daily average available biomass and average temperature at the location.

feasibility of constructing, operating, and disposing the HRESs over their entire lifespan.

These efforts provide a practical framework that supports decisions and policymaking of different combinations of HRES.

2. Materials and methods

2.1. Study location

The Satjelia island, located in the Sundarbans, has an area of 51.66 km^2 [43] and a large population. According to the previous census, it has 40,189 residents and 9,883 households [43]. The location of the study is shown in Fig. 1. In the analysis, the energy demand was evaluated based on standard electrical equipment found in a rural Indian community which consists of 2,200 households, two primary schools, two high schools, and a primary health centre. The evaluation method follows a standard approach used in previous literatures [14,44,45]. The energy demand for the location under study is provided in the Table 2.

The wind speed data for Satjelia village was obtained from NASA databases [46] and is displayed in Table 3. On the left axis, Fig. 2 illustrates the solar irradiance data along with the clearness index on the right axis. The solar data has been taken from NASA databases [46]. The monthly solar irradiance ranges from 4.125 kWh/m^2/day to 6.121 kWh/m^2/day, with an estimated average annual solar irradiance of 4.847 kWh/m^2/day. The maximum solar irradiance occurs in April, while the lowest irradiance intensity is observed in December. In addition, Fig. 3 illustrates the daily average available biomass [14] on the left axis and the average temperature at the location on the right axis.

2.2. System description

The location of the study is rich in biomass as it is located in the Sundarbans. Also, hydrogen is expected to play a major role in India's NetZero goal by 2070. The Government of India provides intensives for green hydrogen production under the program of National Green Hydrogen Mission, run by Ministry of New and Renewable Energy [47]. This study explores eleven HRES combinations based on biomass energy, hydrogen production and traditional diesel-based energy systems to provide required electricity at the remote location of Sundarbans. Eleven distinct HRES combinations within four main categories have been investigated in this study and presented in Fig. 4.

Among all the combinations the first three combinations (1–3) are partially powered by fossil fuels using DG. The combinations (3–8) are all renewable based HRES and are designed to supply the required electricity of the location of study. The combinations (9–11) are capable of producing hydrogen using a 100 kW polymer electrolyte membrane (PEM) electrolyser along with supplying the required electricity at the location. All the required input parameters for techno-economic analysis are provided in Table A1.

2.3. System components

2.3.1. Photovoltaic array

The electrical power generated by the photovoltaic array can be calculated using the following equation [48]:

$$\dot{W}_{PV} = Z_{PV} \times FD_{PV} \times \left(\frac{\overline{I_T}}{\overline{I}_{T,STC}}\right) \times \left(1 + \beta_t \left(T_C - T_{C,STC}\right)\right) \tag{1}$$

where, Z_{PV} represents rated capacity of PV array, FD_{PV} represents PV derating factor, $\overline{I_T}$ represents solar irradiance incident on the PV array in current time step, $\overline{I}_{T,STC}$ is the incident irradiance at standard test conditions, β_t represents temperature coefficient of power, T_C represents PV cell temperature in the current time step, and $T_{C,STC}$ denotes cell temperature under standard test conditions.

The cell temperature can be estimated using the following equation.

$$T_c = \frac{T_a + \left(T_{C,NOCT} - T_{a,NOCT}\right)\left(\frac{\overline{I_T}}{\overline{I}_{T,STC}}\right)\left(1 - \frac{\eta_{MP,STC}\left(1-\beta_t \times T_{C,STC}\right)}{\tau\alpha}\right)}{1 + \left(T_{C,NOCT} - T_{a,NOCT}\right)\left(\frac{\overline{I_T}}{\overline{I}_{T,STC}}\right)\left(\frac{\beta_t \times \eta_{MP,STC}}{\alpha\tau}\right)} \tag{2}$$

where $T_{C,NOCT}$ represents the nominal operating cell temperature, $T_{a,NOCT}$ represents the atmospheric temperature, $\eta_{MP,STC}$ represents the

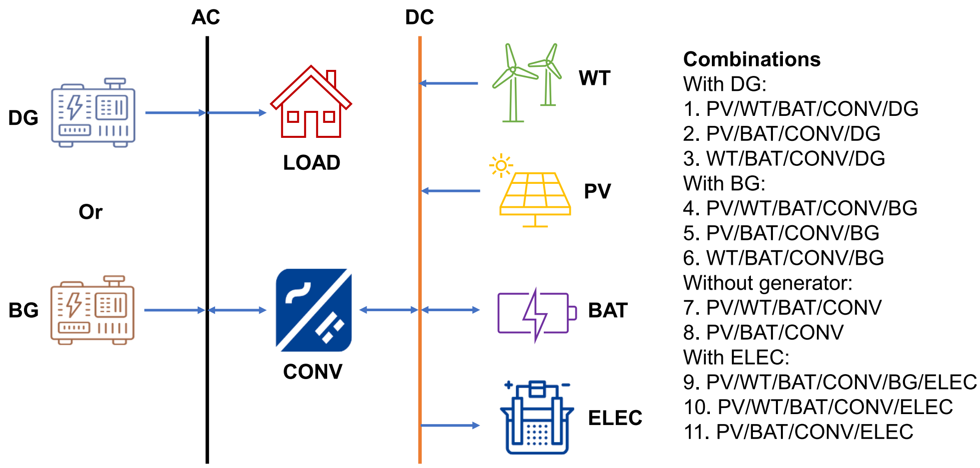

Fig. 4. Combinations of HRES.

maximum power efficiency under standard test conditions, β_t represents the temperature coefficient of power.

The energy output from the PV arrays can be determined using the following equation.

$$E_{PV} = N_{PV} \times \dot{W}_{PV}(t) \times \Delta t \tag{3}$$

where, Δt denotes the time interval, typically taken as one hour.

2.3.2. Wind turbine

The equations below can be used to estimate the power output of wind turbines [48]:

$$\overline{W}_{WT} = \left\{ \begin{array}{c} 0; V \leq V_{cut,in} \\ a \times V^3 - b \times \dot{W}_{rated}; V_{cut,in} \leq V \leq V_{rated} \\ \dot{W}_{rated}; V_{rated} \leq V \leq V_{cut,off} \\ 0; V > V_{cut,off} \end{array} \right\} \tag{4}$$

where the equations provided below can be utilised to determine the values of both 'a' and 'b' [48]:

$$a = \frac{\dot{W}_{rated}}{V^3_{rated} - V^3_{cut,in}} \tag{5}$$

$$b = \frac{V^3_{cut,in}}{V^3_{rated} - V^3_{cut,in}} \tag{6}$$

In the above equations, $\dot{W}_{rated}$, $V_{cut,in}$, V_{rated} and $V_{cut,off}$ represent rated power, cut-in wind speed, rated wind velocity and cut-off wind velocity, respectively.

2.3.3. Battery bank

The reliability of a HRES can be improved by integrating battery storage facilities [49]. These facilities are commonly employed to supply electricity during times of high demand or when renewable sources are unavailable. This investigation examined the effectiveness of lead-acid batteries in storing excess energy during the charging process.

2.3.4. Biomass generator

The electrical efficiency of the biomass generator can be expressed by:

$$\eta_{BG} = \frac{3.6 \times P_{BG}}{\dot{m}_{fuel} \times LHV_{fuel}} \tag{7}$$

where,$\dot{m}_{fuel}$ is the mass flowrate of fuel, P_{BG} is the power output of the generator, and LHV_{fuel} denotes lower heating value of the fuel.

2.3.5. Electrolyser

In this study, PEM type electrolyser has been chosen. PEM electrolyser produces green hydrogen by consuming excess electricity generated by the system. The cathode and anode reactions are provided below [50]:

$$2H^+ + 2e^- \rightarrow H_2 \tag{8}$$

$$H_2O \rightarrow 0.5O_2 + 2H^+ + 2e^- \tag{9}$$

2.4. Economic investigation

In this study, NPC and LCOE were implemented as crucial indicators of economic performance. The comprehensive NPC was evaluated utilising the following equation [51]:

$$NPC = CAP + OM + RC + SL \tag{10}$$

wherein, the summation of total capital cost denoted by CAP, total operating cost signified by OM, total replacement cost represented by RC, and total salvage cost expressed as SL, are considered.

The system's capital cost (CAP) has been characterised by the subsequent relationship [51]:

$$CAP = \sum_{k=1}^{Ncomp} N_k CAP_k \tag{11}$$

where, N_k is the number of components in the system and CAP_k is the capital cost of kth component.

The computation of the system's operating and maintenance cost (OM) has been determined by the following equation [51]:

$$OM = \sum_{k \in comp} \sum_{y=1}^{T_{Proj}} \frac{1}{\left[1 + \left(\frac{d_n - f_r}{1 + f_r}\right)\right]^y} N_k \times OM_k \tag{12}$$

where OM_k denotes the operation and management cost of the kth component, d_n signifies the actual discount rate in percentage, f_r represents the inflation rate in percentage, and T_{Proj} stands for the projected duration of the project in years.

The estimation of the system's replacement cost (RC) can be determined by the subsequent equation [51]:

$$RC = \sum \frac{1}{\left[1 + \left(\frac{d_n - f_r}{1 + f_r}\right)\right]^{T_k}} N_k \times RC_k \tag{13}$$

where T_k and RC_k are total lifetime of the component (years) and total

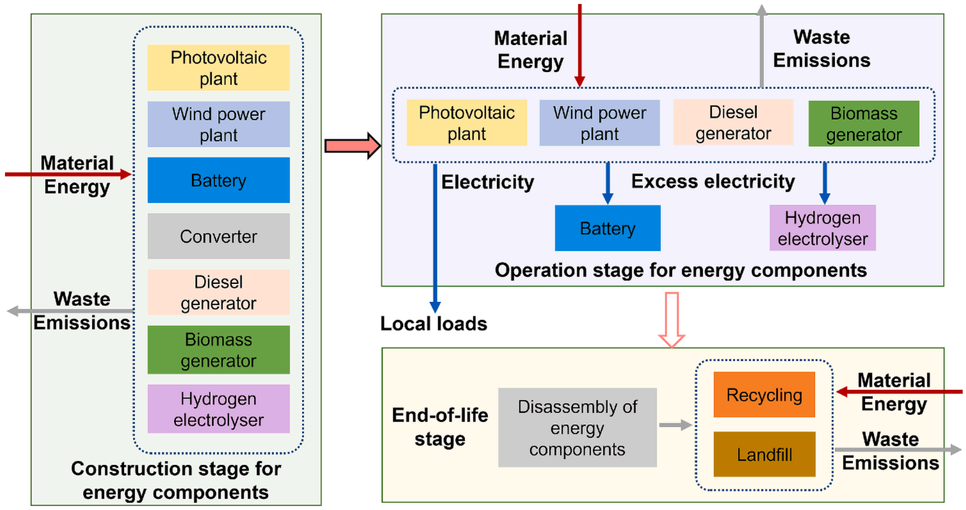

Fig. 5. System boundaries of the HRES used for LCA.

replacement cost of the component, respectively.

The calculation of the system's overall salvage cost (SL) is determined by the subsequent equation [51]:

$$SL = \sum_{k \in comp} \frac{1}{\left[1 + \left(\frac{d_n - f_r}{1 + f_r}\right)\right]^{T_k}} \times \frac{T_{k,rem}}{T_k} \times N_k \times SL_k \tag{14}$$

where $T_{k,rem}$ indicates the remaining lifespan of the kth component by the end of the project, denoted in years, while SC_k signifies the SL of the same component k.

The total annual cost (C_{annual}) is defined as follows [52]:

$$C_{annual} = NPC \times CRF(d_r, T_{Proj}) \tag{15}$$

wherein, CRF pertains to the capital recovery factor and is computed in the following manner [52]:

$$CRF(d_r, T_{Proj}) = \frac{d_r(1 + d_r)^{T_{Proj}}}{(1 + d_r)^{T_{Proj}} - 1} \tag{16}$$

The LCOE denotes the minimum expenditure necessary to market electrical energy at a break-even rate. This metric can be characterised through the following formulation [51]:

$$LCOE = \frac{C_{annual}}{E_{GEN}} \tag{17}$$

where C_{annual} refers to the complete yearly cost in dollars, while E_{GEN} pertains to the overall yearly electricity output measured in kilowatt-hours (kWh/yr).

2.5. Life cycle assessment

In this study, LCA is implemented to assess the environmental impacts of eleven different combinations of HRES. The LCA approach enables the measurement of a process or product's sustainability by calculating the consumption of raw materials and energy and the release of discharges, waste, emissions into the atmosphere. As defined by ISO 14040 [53] and ISO 14044 [54], LCA evaluates impacts of a product from 'cradle to grave' following four main phases, which are the goal and scope definition, inventory analysis, impact assessment and interpretation.

The goal defined for this LCA study is to compare and verify environmental impacts of different energy components in the HRES and to identify combinations with most environmental sustainability potential. Fig. 5 depicts the system boundaries of the HRES which is also the scope definition for LCA. Three stages of construction, operation, and end of life are included. At the construction stage, input flows include the raw materials and fuels acquired for manufacturing component, as well as the electricity and heat consumed for assembling the system. Waste generated during the construction only considers the impacts of the waste itself and no further impacts from waste treatment are considered. The operation stage includes raw material and energy required for producing the power, such as for PV system where solar energy is used as an input stream. Operation stage takes into account the materials consumed during the maintenance and cleaning processes. At the end-of-life stage, it is assumed that the energy components will be dissipated and landfilled. Each stage is connected by the transportation, the impacts of which are involved in the related database of energy components. The functional unit of this LCA study is defined as the environmental impacts associated with supplying electricity throughout one year by HRES.

Table 4
Capacities and lifetime of the reference components.

Component	PV	WT	DG	BG	CONV	ELEC
Capacity (kW)	570	800	84	84	500	1000
Lifetime (year)	30	Moving parts: 20 Fixed parts: 40	20	20	15	10

The life cycle inventory analysis as the second phase of LCA needs to collect the data aligned with the targets defined in the goal and scope. Typically, the required input data is necessary to be specific to each component's construction, operation, and disposal stages. Due to the constrains of data availability, inventory data could also be collected from commercial LCA database, literatures, and manufacturer report data, etc. When utilising the inventory data of a reference component, the input streams will be scaled through a non-linear approach as equation (18)[55]:

$$In_B = In_A \times \left(\frac{Capacity_B}{Capacity_A}\right)^f \tag{18}$$

where In_A and In_B represent the amounts of input materials and energy for the reference components and the built components, respectively, while $Capacity_A$ and $Capacity_B$ are respective capacities of the reference and designed components, and f is the scale factor which is set at 0.6 as the same as the economy of scale factor. The power capacities and lifetime of the reference PV, WT, DG, BG, CONV, and ELEC are listed in Table 4.

Life cycle inventory data of manufacturing PV plant, converter, and

Table 5
Operation data for generating 1 kWh electricity from different components [56].

Component	Inputs	Unit	Other outputs	Unit	Process in Ecoinvent
PV	Solar energy	MJ	Water	m^3	Electricity production, photovoltaic, 570kWp open ground installation, multi-Si
	Tap water	kg	Wastewater	m^3	
WT	Wind energy	MJ	Waste mineral oil	kg	Electricity production, wind, <1MW turbine, onshore
	Lubricating oil	kg			
DG	Diesel	L	Emissions to air [a]	kg	Diesel, burned in diesel-electric generating set
	Lubricating oil	kg	Waste mineral oil	kg	
BG	Biogas	L	Emissions to air [b]	kg	Heat and power co-generation, biogas, gas engine
	Lubricating oil	kg	Waste mineral oil	kg	

[a] The emissions include benzene, benzopyrene, cadmium, CO_2, CO, copper ion, N_2O, mercury, ethane, non-methane volatile organic compounds, nickel, nitrogen oxides, PM2.5, selenium, SO_2, zinc.
[b] The emissions include CO_2, CO, N_2O, SO_2, methane, non-methane volatile organic compounds, nitrogen oxides, platinum.

wind power plant are sourced from LCA data in Ecoinvent 3.9.1 [56] under the processes of "*photovoltaic plant construction, 570kWp, multi-Si, on open ground*", "*inverter production, 500 kW*", "*wind power plant, 800 kW, fixed parts*" and "*wind power plant, 800 kW, moving parts*", respectively. Details of the input flows for construction of diesel and biomass generators, and PEM water electrolysis plant are cited from references [28,57], which are given in the Appendix as Tables A2–A3. It is assumed that both diesel generator and biomass generator apply the same reference component and input streams. For the production of batteries used to store excess electricity, life cycle inventory data of 1 kg lead acid battery production from Ecoinvent 3.9.1 is employed. The total material and energy consumed for manufacturing the required mass of battery could be calculated by multiplying 1 kg inventory data with the battery mass derived from the model. The battery will be replaced by every 5 years.

During the operation stage, electricity and hydrogen are two main products from HRES. In the configuration of HRES, PV, WT, DG, and BG are the four components used to produce electricity. The battery is used to store excess electricity, meanwhile ELEC will generate hydrogen using this excess electricity. Therefore this study only considers the operation data for PV, WT, DG, BG, and ELEC. The main inputs and outputs are listed in Table 5, based on generating 1 kWh of electricity from different energy components. The exchanges refer to specific electricity production process from the Ecoinvent database. For the operation of ELEC, 9 kg H_2O is required to produce 1 kg H_2 based on the stoichiometry equation of water splitting, and 46.4 kWh of electricity is necessary for H_2 production from the results of modelling. The transportation data have been involved in the cited process data sourced from Ecoinvent [56] and not separately compiled here.

For the LCIA stage, the ReCiPe 2016 midpoint method was utilised, which translates the resource extractions, consumption, and substance emissions from life cycle inventory analysis into 18 environmental impacts by using the software SimaPro 9.5. These environmental effects include climate change, ozone depletion, freshwater and marine eutrophication, human toxicity, land use, fossil resource scarcity, and water use, etc.

Table 6
Optimised design results of each component in eleven HRES.

HRES	PV	WT	DG	BG	BAT	CONV	ELEC
1	1,366 kW	315 kW	710 kW	–	4,264 strings	495 kW	–
2	1,566 kW	–	710 kW	–	4,391 strings	406 kW	–
3	–	963 kW	710 kW	–	1,273 strings	470 kW	–
4	1,344 kW	364 kW	–	500 kW	4,419 strings	502 kW	–
5	1,811 kW	–	–	500 kW	5,229 strings	463 kW	–
6	–	2,441 kW	–	500 kW	4,251 strings	789 kW	–
7	4,173 kW	743 kW	–	–	6,184 strings	692 kW	–
8	6,600 kW	–	–	–	8,218 strings	1,090 kW	–
9	2,459 kW	2,459 kW	–	500 kW	1,046 strings	522 kW	100 kW
10	6,902 kW	865 kW	–	–	5,406 strings	865 kW	100 kW
11	11,112 kW	–	–	–	5,884 strings	1,116 kW	100 kW

3. Results and discussion

3.1. Technical assessment

In this sub-section, the technical performances of eleven HRES combinations are discussed in detail. Technical performance parameters such as optimised design configuration, renewable fraction, diesel requirement, electricity production, excess electricity generation, unmet load (kWh/yr), capacity shortage, and hydrogen production are considered in the technical performance investigation. The Tables 6 and 7 show the respective optimised design and technical performances results of eleven investigated HRES. It is observed that among the three partially non-renewable HRES combinations, combination 1 has the highest renewable fraction (86.7 %), followed by combination 2 (78.7 %) and combination 3 (41.7 %), respectively. The lowest diesel consumption is found in combination 1 (62,747.04 L/yr). The electrolyser-integrated combination 11 has the maximum PV capacity (11,112 kW). In terms of battery capacity, combination 8 has the maximum number of strings (8,218). In terms of wind turbine capacity, combination 9 has the highest capacity (2,459 kW). The annual hydrogen production of all three electrolyser-integrated systems is mostly same. Regarding excess electricity generation, combination 11 has the maximum (87.4 %), and combination 3 has the lowest (17.40 %). It should be noted that producing a significant excess of electricity necessitates the allocation of extra storage space, which can result in a greater LCOE and a heavier economic burden.

3.2. Economic results

Fig. 6 presents the NPC and LCOE for various combinations examined at the study site. The economic analysis shows that combination 1, comprising PV/WT/BAT/CONV/DG, yields the lowest LCOE (0.319 $/kWh) and NPC (6.81 M$). However, among the fully renewable-based configurations, combination 4, incorporating PV/WT/BAT/CONV/BG, offers the minimum LCOE (0.388 $/kWh) and NPC (8.28 M$). Among the electrolyser-integrated systems, combination 9, combining PV/WT/BAT/CONV/BG/ELEC, exhibits the lowest LCOE (0.547 $/kWh) and NPC (11.7 M$). On the other hand, combination 11 demonstrates to be the most expensive option, with the highest LCOE (0.8005 $/kWh) and NPC (17.08 M$).

Fig. 7 depicts the capital costs for the eleven system combinations, along with a breakdown of the capital costs for the different components

Table 7
Technical analysis results of eleven HRES.

HRES	Renewable fraction (%)	Diesel requirement (L/yr)	Electricity production (kWh/yr)	Excess electricity (kWh/yr)	Unmet load (kWh/yr)	Capacity shortage (%)	Hydrogen production (kg/yr)
1	86.7	62,747	2,668,996	789,518 (29.6 %)	0	0	–
2	78.7	97,956	2,728,841	852,437 (31.20 %)	0	0	–
3	41.7	279,545	2,111,376	366,985 (17.40 %)	0	0	–
4	100	0	2,676,406	788,699 (29.5 %)	346	0.045	–
5	100	0	2,978,311	1,063,164 (35.7 %)	276	0.044	–
6	100	0	3,385,252	1,551,891 (45.8 %)	1,026	0.096	–
7	100	0	7,723,210	5,338,776 (73.9 %)	897	0.099	–
8	100	0	10,021,897	8,081,673 (80.6 %)	1,071	0.099	–
9	100	0	5,497,177	3,531,394 (64.2 %)	138	0.008	4,105
10	100	0	11,511,978	9,444,538 (82 %)	722	0.091	4,109
11	100	0	16,871,574	14,745,051 (87.4 %)	873	0.095	4,110

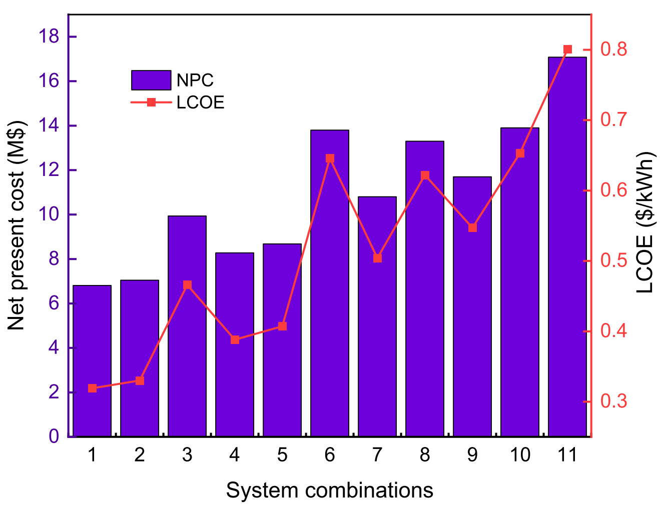

Fig. 6. NPC and LCOE of different system combinations.

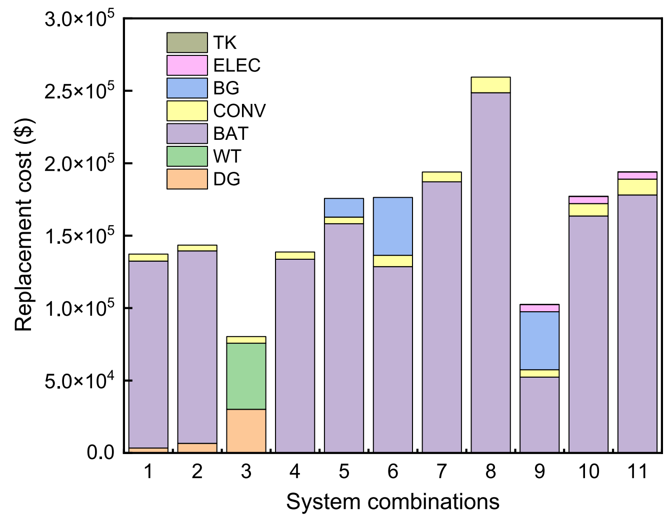

Fig. 8. Replacement cost of different system combinations.

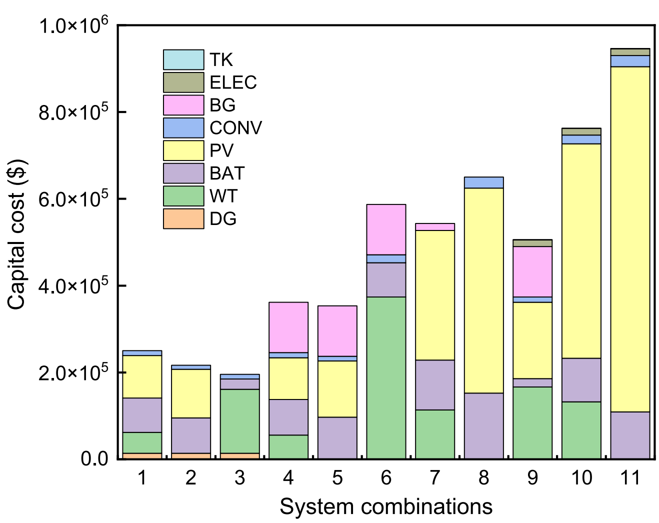

Fig. 7. Capital costs of different system combinations.

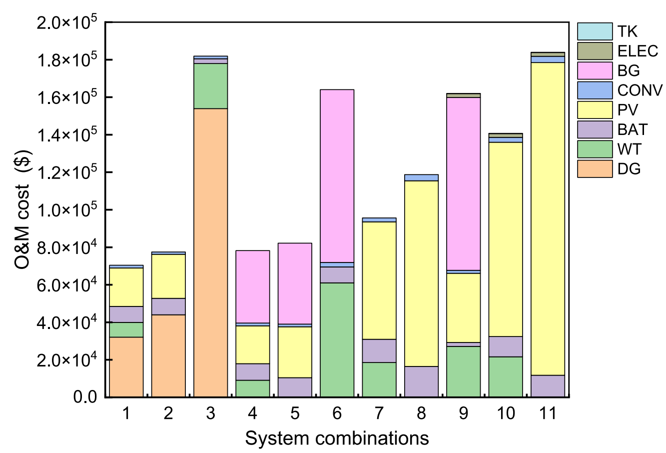

Fig. 9. O&M cost of different system combinations.

used in each combination. From the Fig. 7, it is evident that combination 3 has the lowest total capital cost requirement among all the combinations. It is observed that WT (75.34 %) contributed the highest capital cost, followed by BAT (12.07 %), DG (7.01 %), and CONV (5.47 %), respectively, for combination 3. Among the completely renewable systems, combination 5 has the lowest capital cost requirement, with the highest capital cost contribution from PV (36.66 %), BG (32.83 %), BAT (27.47 %), and CONV (3.04 %), respectively. It is also found that the combination 9 has the lowest capital cost requirement among the electrolyser integrated systems. PV component contributed the highest capital cost (34.77 %), followed by WT (32.91 %), BG (22.93 %), BAT (3.84 %), ELEC (3.06 %), CONV (2.39 %), and tank (TK) (0.10 %), respectively for combination 9. Combination 11 has the highest capital cost requirement, with PV contributing the most (84.03 %).

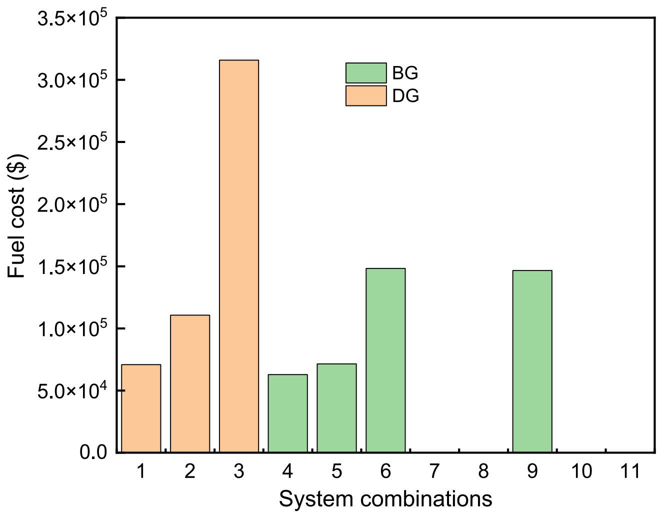

Fig. 10. Fuel cost of different system combinations.

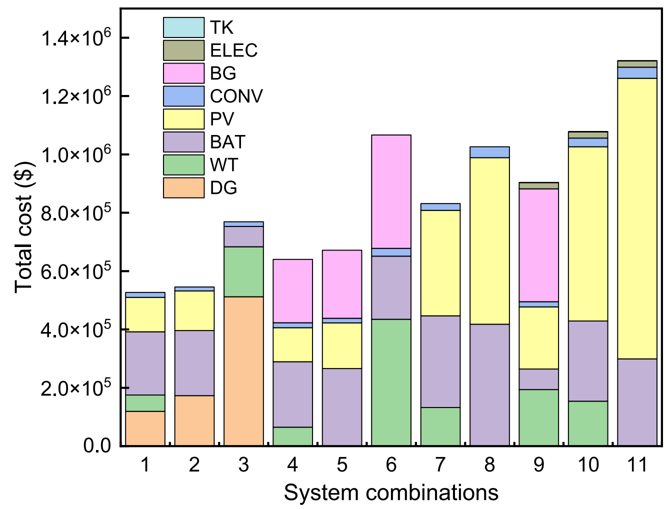

Fig. 12. Total cost of different system combinations.

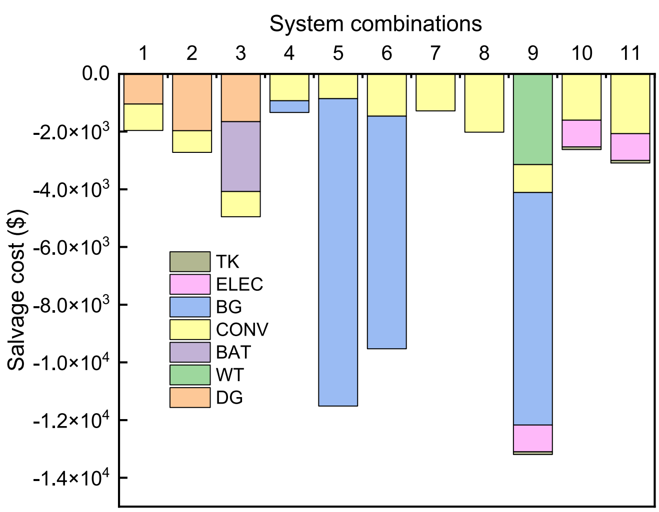

Fig. 11. Salvage cost of different system combinations.

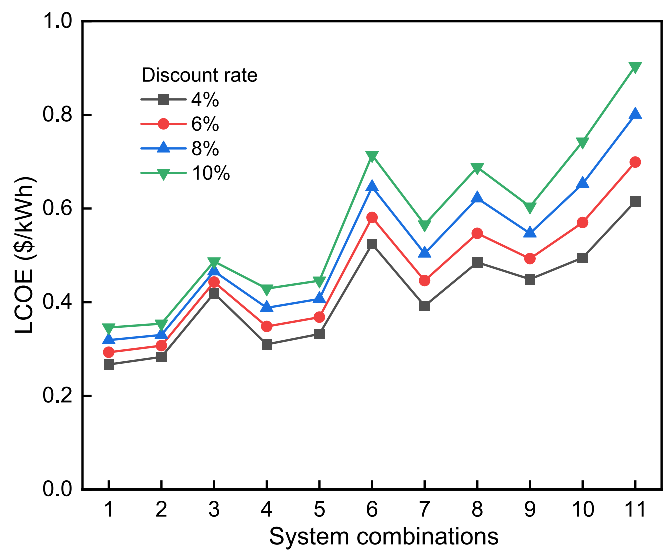

Fig. 13. Effect of discount rates on LCOE of different system combinations.

It is essential to consider that some system components may need replacement over the lifespan of the project. Fig. 8 depicts the replacement cost of all the eleven HRES combinations. It is observed that combination 3 has the lowest replacement cost among all the investigated combinations, with the highest replacement cost contribution coming from WT (56.80 %), followed by DG (37.44 %), and CONV (5.76 %). Among the completely renewable systems, combination 9 has the lowest replacement cost, with BAT (51.03 %) contributing the most, followed by BG (39 %), CONV (5.01 %), ELEC (4.80 %), and TK (0.16 %), respectively. Among all the investigated systems, combination 8 has the highest replacement cost, with BAT contributing 95.86 % and CONV 4.14 %, respectively.

Fig. 9 depicts the operation and management costs of all the HRES combinations studied. The results suggest that combination 1 exhibits the least operating and maintenance (O&M) costs when compared to all the other combinations. In combination 1, DG has the highest O&M cost contribution (45.52 %), followed by PV (29.09 %), BAT (12.11 %), WT (11.18 %), and CONV (2.11 %). Among all the completely renewable systems, combination 4 has the lowest O&M costs, with BG contributing the most (49.35 %), followed by PV (25.78 %), WT (11.64 %), BAT (11.30 %), and CONV (1.93 %). Combination 11 has the highest O&M costs among all the combinations, with PV contributing the most (90.62 %), followed by BAT (6.40 %), CONV (1.82 %), ELEC (1.09 %), and TK (0.07 %), respectively.

The Fig. 10 shows the fuel costs of different system components. It is important to note that only BG or DG integrated systems consume fuel. It is observed from the figure that among the DG integrated systems, combination 3 has the highest cost due to diesel consumption ($315,885.86), followed by combination 2 and combination 1, respectively. Among the BG integrated systems, combination 4 has the lowest cost due to biomass consumption. The Fig. 11 depicts the salvage costs of different system combinations. It is observed that among the DG integrated systems, combination 1 yields the lowest salvage cost, of which DG contributes 53.20 % and CONV contributes 46.80 %, respectively. Combination 4 yields the lowest salvage cost among all the systems investigated in this study, of which CONV contributes 69.65 % and the rest is contributed by BG. It is also observed that combination 9 yields the maximum salvage costs, of which BG contributes the highest percentage (61.13 %), followed by WT (23.82 %), CONV (7.33 %), ELEC (7.02 %), and TK (0.70 %), respectively.

The Fig. 12 depicts the total cost of different combinations investigated in this study. It is observed that combination 1 yields the lowest total cost, of which BAT contributes the maximum (41.12 %), followed by DG (22.59 %), PV (22.43 %), WT (10.65 %), and CONV (3.21 %), respectively. Among the completely renewable-based system

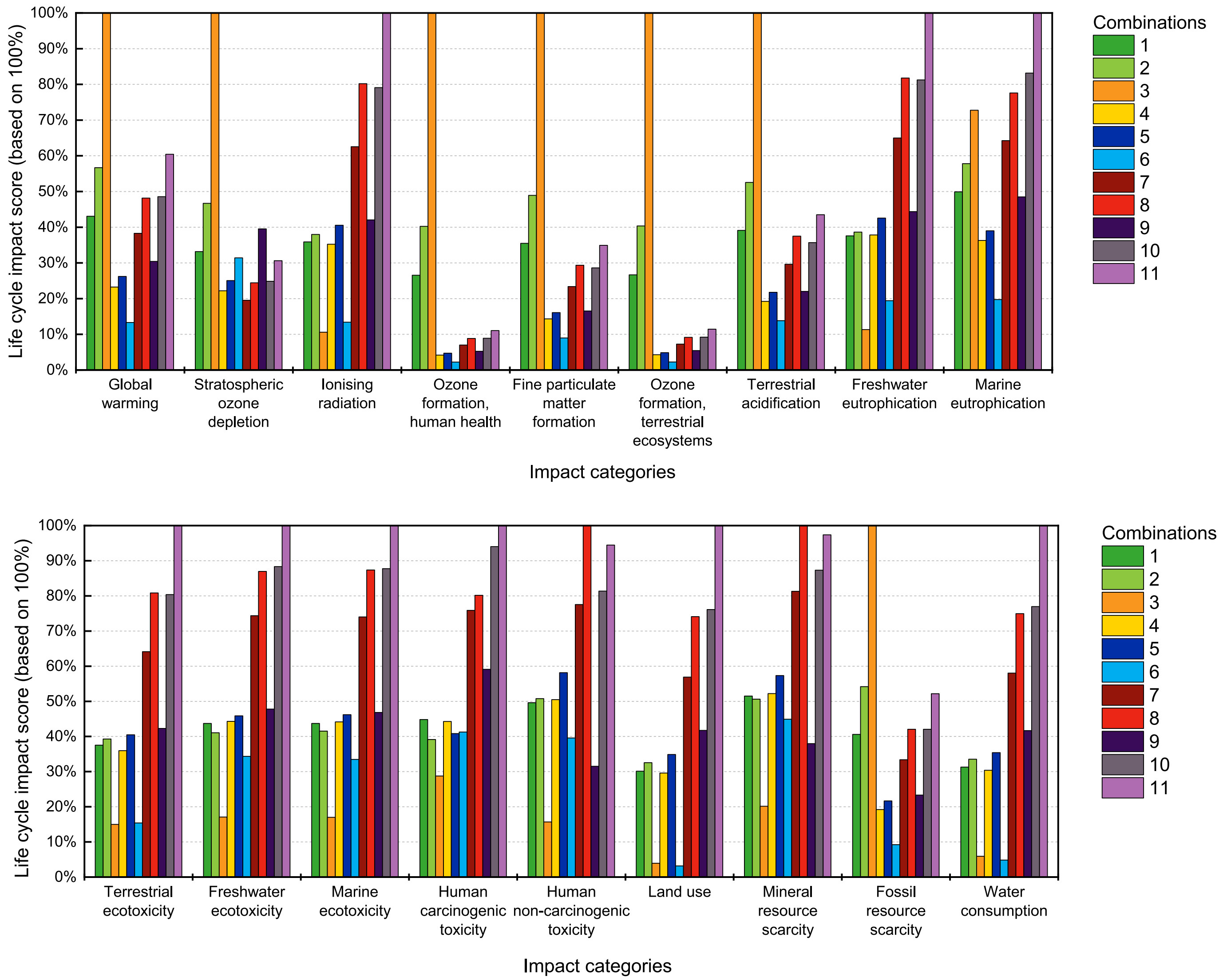

Fig. 14. Life cycle environmental impacts of different HRES combinations based on 100% score.

combinations, combination 4 yields the lowest total costs, of which BAT contributes 35.09 %, followed by BG (33.92 %), PV (18.18 %), WT (10.13 %), and CONV (2.68 %), respectively. It is also found that combination 11 yields the maximum total costs, of which PV contributes the most (72.79 %), followed by BAT (22.64 %), CONV (2.89 %), ELEC (1.62 %), and TK (0.05 %).

The Fig. 13 depicts the effect of discount rates on LCOE of different system combinations. As the rate of discount varies from 4 % to 10 %, the LCOE of different system combinations also increases. It is observed that the combination 1, comprising PV/WT/BAT/CONV/DG yields lowest LCOE compared to other systems across all the scenarios and yields the lowest LCOE of 0.267 $/kWh at discount rate of 4 %. On the contrary, the combination 11 is found to be the most expensive option, with the highest LCOE of 0.904 $/kWh at discount rate of 10 %.

3.3. Environmental impacts

This section discusses the environmental impacts obtained through LCIA method ReCiPe 2016 midpoint for eleven HRES combinations. These impacts are firstly compared across all combinations, as shown in Fig. 14 where the combination with the largest impact value is assigned a weight of 100 %. Then the smaller impact values of other combinations are converted as a percentage of the largest value. The highest values of each impact category are found to be attributed to three different combinations: combination 3 (WT/BAT/CONV/DG), combination 8 (PV/BAT/CONV), and combination 11 (PV/BAT/CONV/ELEC). Although the combination 3 utilises the wind turbine, it only has 41.7 % renewable energy penetration. With the highest requirement of diesel, i. e., 279,545 L per year, it leads to the largest impacts values for global warming, ozone depletion and formation, particulate matter formation, soil acidification, and fossil resource consumption. These impacts are directly associated with GHG when using the diesel. Additionally, the combustion of diesel could result in other hazardous emissions to the air as detailed in Table 5, causing severe impacts on both the atmosphere and terrestrial environment.

Combination 11 in which PV dominates the electricity generation and ELEC produces the most hydrogen, is found to have the maximum impacts in most categories. These impact categories are primarily related to the ionising irradiance, freshwater and marine ecosystem. It is worth noting that besides the water consumed in the electrolyser, the operation of PV also uses significant amounts of water for cleaning the PV panels and releases wastewater directly into the environment. Due to the large-scale mounting required to install the PV panels on open ground, this combination also contributes most to the impact on the land use, which limits its application in small areas. These impacts should not be neglected for its deployment from a life cycle perspective, even

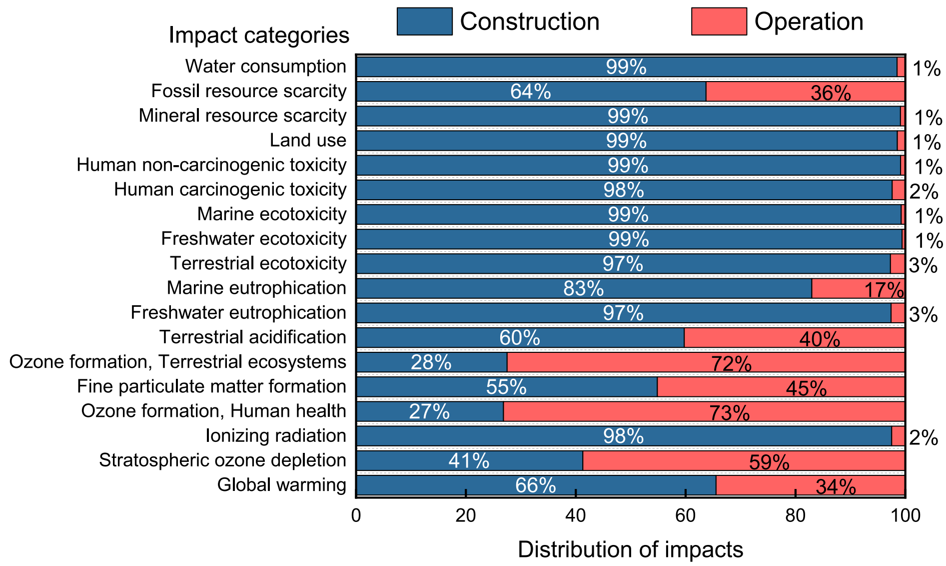

Fig. 15. Distribution of impacts from construction and operation stages.

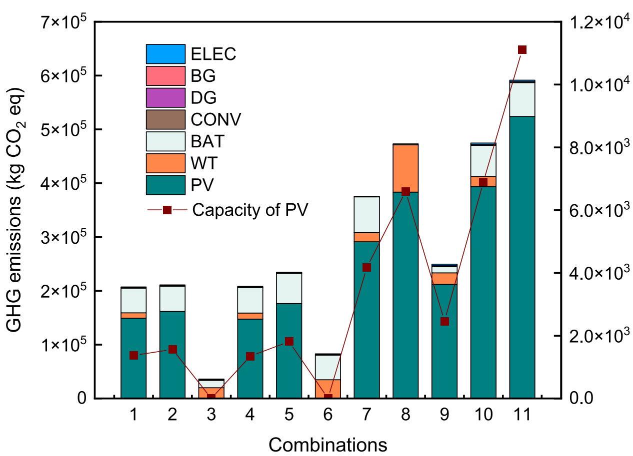

Fig. 16. GHG emissions from construction stage of different HRES.

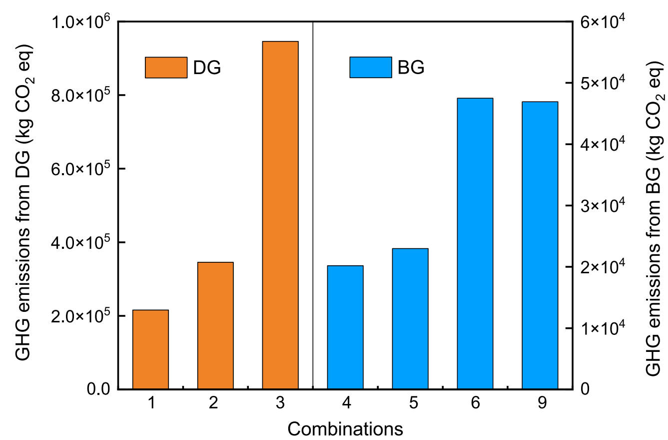

Fig. 17. GHG emissions of DG and BG during their operation stage.

though this combination has achieved 100 % renewable energy production. Another factor influencing the final impacts comes from the energy storage, as reflected in the combination 8. In this combination, the maximum use of battery increases the impacts associated with human non-carcinogenic toxicity and mineral resource consumption. To further offset the impacts from fossil-fuel consumption, the battery should be applied properly and recycled effectively.

The total impacts are then broken down into the percentages attributed to the construction and operation stages, as shown in Fig. 15. Overall, the construction stage contributes more to the impacts than the operation stage, except for the impacts from ozone formation and depletion which account lower than 50 %. Significant impacts from the operation stage keep consistent with those caused most by combination 3, proving that the operation of diesel brings less environmental benefits. This distribution figure reveals the environmental challenges related to constructing large-scale HRES, as these impacts will obviously increase with the larger size of whole system. More mitigation technologies and environmentally sustainable materials should be considered for the building of the energy components.

The results of GHG emissions from the construction stage are explained in detail in Fig. 16 to find the specific impact from different energy components. For combinations with PV, the manufacturing of PV accounts most to the GHG emissions from construction stage, which

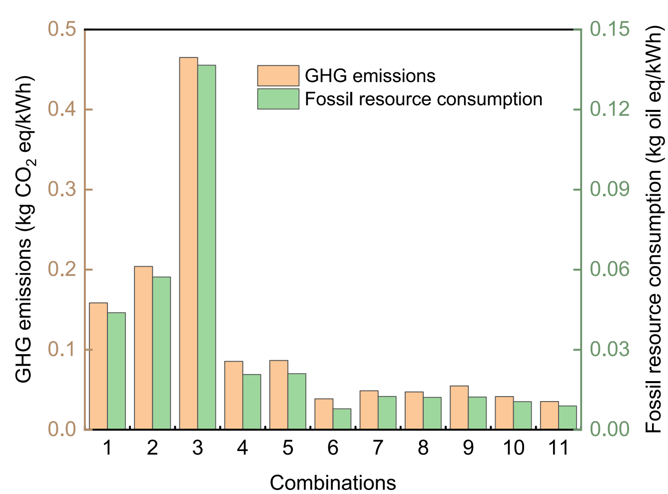

Fig. 18. GHG emissions and fossil resource consumption of per kWh electricity production.

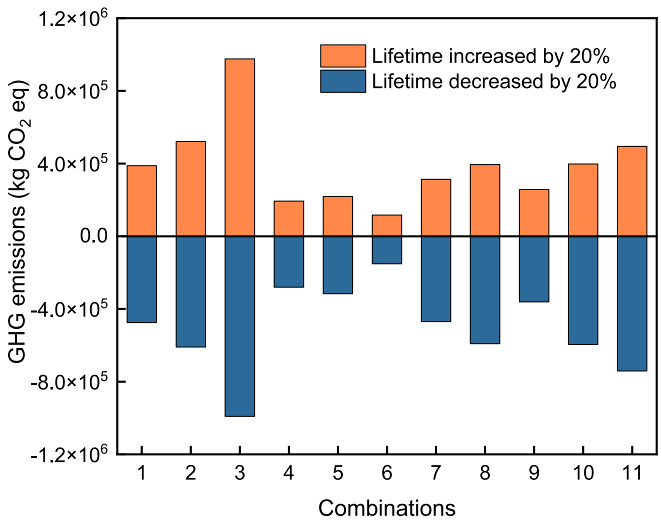

Fig. 19. Impacts of components' lifetime on GHG emissions.

ranges 148 to 524 tons of equivalent CO_2 when the capacity of PV system increases from 1,344 kW to 11,112 kW. The construction and assembly of battery and wind turbine are other two significant sources of GHG emissions. For the operation stage, the majority of the GHG emissions is from the combinations that involve diesel and biomass generators, as the GHG emissions from renewable energy components are negligible. Fig. 17 shows the comparison between GHG emissions from the operation of DG and BG. The combustion of diesel in DG is identified as a major GHG hot spot and emits 20 times more GHG emissions than biogas utilisation in BG. Although a part of GHG emissions is still sourcing from combustion of biogas, BG could offset these emissions compared to traditional DG, given that biomass is a carbon neutral material.

As the primary objective of HRES in this study is to supply electricity to locals, it is crucial to understand the specific GHG emissions and fossil fuel consumption based on per kWh electricity output. Fig. 18 displays these two results across all combinations. With higher rates of fossil depletion, combinations 1–3 exhibit the higher specific GHG emissions (0.16 to 0.47 kg CO_2 eq/kWh) and fuel consumption (0.04 to 0.14 kg oil eq/kWh) compared to other combinations. Combination 2 ranks the second highest in terms of specific GHG emissions and fossil depletion with 78.7 % of electricity generation from renewable sources. The lowest specific impacts are observed in combinations 6 and 11, with both GHG emissions and fuel consumption less than 0.04 kg CO_2 eq/kWh and 0.01 kg oil eq/kWh, respectively. The combination 6 eliminates the use of PV and DG generators, indicating the most significant reduction in GHG emissions and fossil utilisation. These results suggest that when planning a HRES with small capacity, WT and BG could be considered.

The lifetime of energy components in HRES is selected to be increased and decreased by 20 % with respect to the reference lifetime, to investigate its effects on the GHG emissions. Fig. 19 presents results of GHG emissions, in which the negative value shows the results under decreased components' lifetime. An increase in lifetime reduces GHG emissions of per year from the construction stage, whereas reduced lifetime results in more frequent component replacement and higher demands in the material and energy used for the construction, thereby increasing the GHG emissions. Combination 11 shows particularly sensitive to the changes of lifetime, due to its largest PV installation during the construction stage, greatly impacted by the varied lifetime. Moreover, based upon the changes in GHG emissions, decreased lifetime has more significant influence on the impacts. This highlights the importance of designing energy components with extended lifetime, which could decrease the life cycle GHG emissions.

Table 8
Comparisons with other systems.

Refs.	System combinations	Location	LCOE
This study	PV/WT/BAT/CONV/DG	Satjelia, India	0.319 $/kWh
This study	PV/WT/BAT/CONV/BG/ELEC	Satjelia, India	0.547 $/kWh
[14]	PV/BG/BAT/CONV	Sidhwanbet, India	0.362 $/kWh
[58]	WT/PV/FC/BAT/CONV/ELEC	Kanur, India	0.189 $/kWh
[59]	PV/BG/BAT/CONV	Delhi, India	0.20 $/kWh
[60]	PV/WT/DG/BAT	Saint Martin, Bangladesh	0.1724 $/kWh
[61]	PV/BAT/DG	Kutubdia Island, Bangladesh	0.179 $/kWh
[62]	PV/DG/BAT	Ghana	0.38 $/kWh
[63]	PV/WT/BAT	Mardan, Pakistan	0.91 $/kWh
[64]	HT/WT/PV/DG	Isle of Rum, United Kingdom	0.99 $/kWh*
[65]	HT/ELEC/CONV/PV	Ouenskra, Morocco	0.147 $/kWh
[66]	PV/WT/BAT/DG	Rural village, Srilanka	0.30 $/kWh
[67]	PV/ELEC/FC/CONV	Kalat, Pakistan	0.433 $/kWh
[8]	PV/WT/Grid	Dinajpur, Bangladesh	0.03 $/kWh
[68]	PV/WT/Grid	Kunder Char, Bangladesh	0.0436 $/kWh
[69]	PV/BG/BAT	Dahan-i-Garmab, Afghanistan	0.29 $/kWh
[70]	PV/Hydro power/BAT/CONV	Hurawalhi, Maldives	0.1189 $/kWh
[71]	PV/Hydro power/CONV	Nepal	0.067 $/kWh

* A GBP-USD exchange rate of 1.3 (as of Oct 2024 [72]) was used to convert £0.76/kWh to $0.99/kWh.

To minimise the impacts related to global warming, ozone formation and depletion, and fossil resource scarcity, the configuration of HRES should avoid the use of DG. Even hydrogen serves as an effective storage medium for renewable energy, the size of renewable energy system should be matched to the capacity of hydrogen electrolyser to prevent excess electricity generation and substantial installation of energy system which could cause larger life cycle impacts. When combining the environmental results with cost results, combination 9 (PV/WT/BAT/CONV/BG/ELEC) appears more environmentally and cost effective compared to other combinations. Besides achieving 100 % renewable energy conversion, this combination also promotes local biomass resources and produces hydrogen, with a relatively lower LCOE and total cost.

3.4. Comparison with other systems

In this subsection, the results of the proposed systems are compared with the results of the other systems located in the countries near the studies area as in Table 8. The PV/WT/BAT/CONV/BG/ELEC and PV/WT/BAT/CONV/DG systems can yield LCOEs of 0.547 $/kWh and 0.319 $/kWh, respectively. This result is comparable to the other studies. However, a similar type of system was not found in the literature. It can be inferred that with increasing component-level hybridization, the LCOE of the system might increase. Also, the capital cost considered for different components highly influence the LCOE value. The choice of components selection depends on the availability of the energy resources based on their geographic location.

3.5. Implication in HRES design

India is committed to achieve Net Zero target by year 2070. India's long term low carbon development strategy includes low-carbon development of electricity systems consistent with development [73].

In this regard, renewable HRES configurations deployment particularly in the remote locations can be useful to achieve long term decarbonisation goal. The results obtained from the study could be useful in microgrid design and energy planning particularly in the remote areas of India.

HRES design and planning based on using local energy resources such as biomass availability, solar energy availability, wind speed etc should be considered in designing microgrids in remote locations in India. It is important to consider the local energy demands while designing HRES for the remote and rural locations. Collaboration between private players and government entities in developing HRES in remote areas could be considered for large scale deployment. Green financing could be a solution for large scale HRES deployments in remote and rural areas using public–private partnerships.

4. Conclusion

In this paper an attempt has been made to investigate multiple off-grid HRES configurations to meet the energy requirements of a village community located in the Sundarbans, India. The study employed technical, economic, and LCA methods to evaluate eleven HRES combinations that incorporate PV, WT, BAT, DG, BG, CONV, and ELEC. Furthermore, the objective of this research is aligned with United Nations SDG No. 7, which strives to achieve “Affordable and Clean Energy”. To determine the optimal HRES combinations, the LCOE was minimised during the sizing of the systems and ReCiPe 2016 midpoint method has been utilised for life cycle impact assessment. The major findings of this study are provided as follows:

- HRES comprising PV, WT, BAT, CONV, and DG, has the lowest LCOE (0.319 $/kWh) and NPC (6.81 M$) among all eleven combinations.
- Among the partially fossil powered HRES, integrating both PV and WT could reduce diesel consumption and improve the renewable fraction to 86.7 %.
- For HRES incorporating DG, the operation of generator accounts for a significant proportion of impacts from global warming, ozone formation and depletion, and fossil resource scarcity, suggesting that the combination of HRES should avoid use of DG.
- For HRES involving PV, PV contributes most to the GHG emissions of construction stage, meanwhile its operation increases life cycle impacts on ionising radiation, and freshwater and marine ecosystem.
- HRES with combination of PV/WT/BAT/CONV/BG/ELEC is considered to have most environmental and economic effects, as it achieves sufficient penetration of renewable energy and production of hydrogen, with a lower LCOE and total cost.

This study provides valuable insights into the design and optimisation of a proposed HRES based on minimising LCOE, highlighting its potential to meet the energy demands of remote locations in India. The reliability of this study depends on the metrological conditions, electrical load requirements, and local renewable energy availability. Also, the economic calculations heavily rely on the assumptions and capital costs of the components. In future studies, the focus will be on the control mechanisms and resilience of the proposed HRES combinations. It will be interesting to optimise the HRES combinations employing multi-objective optimisation using machine learning algorithms. The results could be useful in microgrid design and energy planning particularly in the remote areas in India. The study shows promise in addressing the challenges associated with the inconsistent and unreliable supply of electricity in remote areas in India.

CRediT authorship contribution statement

Dibyendu Roy: Writing – review & editing, Writing – original draft, Software, Methodology, Investigation, Visualization, Formal analysis, Data curation, Conceptualization. **Ruiqi Wang:** Writing – review & editing, Writing – original draft, Software, Methodology, Formal analysis, Investigation, Visualization, Funding acquisition. **Sumit Roy:** Writing – review & editing, Investigation, Project administration, Conceptualization. **Andrew Smallbone:** Writing – review & editing, Supervision, Investigation, Funding acquisition. **Anthony Paul Roskilly:** Writing – review & editing, Supervision, Resources, Funding acquisition.

Table A1
Input parameters for technoeconomic analysis.

Component	Parameters	Data	Ref
PV	Derating factor	80 %	[74,75]
	Temperature coefficient	−0.5/°C	
	Efficiency	13 %	
	Operating Temperature	47 °C	
	Rated current	5.98A	
	Capital cost	925 $/kW	
	Replacement cost	800 $/kW	
	O&M cost	15 $/kW	
	Lifetime	25 years	
WT	Hub height	20 m	[74]
	Rated wind speed	12.5 m/s	
	Start-up wind speed	2.5 m/s	
	Diameter of rotor	3.35 m	
	Capital cost	1980 $/kW	
	Replacement cost	980 $/kW	
	O&M cost	25 $/year	
Battery	Voltage rating	12 V	[74]
	Capacity ratio	0.403	
	Roundtrip efficiency	80 %	
	Minimum state of charge	20 %	
	Initial state of charge	100 %	
	Capital cost	240 $/unit	
	Replacement cost	190 $/unit	
	O&M cost	2.0 $/year	
Converter	Inverter efficiency	95 %	[76]
	Rectifier efficiency	95 %	
	Capital cost	300 $/kW	
	Replacement cost	300 $/kW	
	O&M cost	3 $/year	
BG	Power rating	500 kW	[77]
	Fuel cost	100 $/t	
	Biogas density	0.720 kg/m^3	
	Capital cost	3,000 $/unit	
	Replacement cost	1,250 $/unit	
	O&M cost	0.10 $/hour	
Electrolyser	Efficiency	85 %	[76]
	Capital cost	1,500 $/unit	
	Replacement cost	1,000 $/unit	
	O&M cost	20 $/year	
Hydrogen tank	Capacity	1 kg	[76]
	Capital cost	600 $/unit	
	Replacement cost	450 $/unit	
	O&M cost	10 $/year	
Diesel generation	Capital cost	525 $/kW	[62]
	Replacement cost	509 $/kW	
	O&M cost	0.028 $/hour	
	Minimum load ratio	25 %	
	Fuel curve intercept	3.25 Lt/hour	
	Fuel curve slope	0.236 L/hour/kW	
	Lower heating value of diesel	43.2 MJ/kg	

Table A2
Installation data for 84 kW diesel and biomass generators [28].

Inputs	Amount
Materials/fuels	
Aluminium alloy, $AlMg_3$ (kg)	32.79
Aluminium, cast alloy (kg)	30.86
Cast iron (kg)	140.48
Copper (kg)	40.05
Epoxy resin, liquid (kg)	3.27
Ferromanganese, high-coal, 74.5 % Mn (kg)	6.05
Lead (kg)	0.73
Molybdenum (kg)	1.69
Nickel, 99.5 % (kg)	2.66
Pig iron (kg)	179.29
Printed wiring board (kg)	1.45
Silicon carbide (kg)	146.69
Steel, chromium steel 18/8 (kg)	2.54
Steel, low-alloyed (kg)	498.28
Steel, low-alloyed, hot rolled (kg)	121.85
Tin (kg)	0.48
Titanium (kg)	0.36
Zinc (kg)	0.36
Electricity/heat	
Electricity, high voltage (GJ)	19.36
Heavy fuel oil, burned in refinery furnace (MJ)	65.34

Table A3
Manufacturing data for 1 MW PEM water electrolyser plant [57].

Inputs	Amount
Capacity (kW)	1,000
Iridium (kg)	0.75
Platinum (kg)	0.075
Titanium (kg)	528
Aluminium, primary, ingot (kg)	27
Steel, unalloyed (kg)	100
Copper-rich materials (kg)	4.5
Tetrafluoroethylene (kg)	16
Activated carbon, granular (kg)	9
Low alloyed steel (kg)	4,800
High alloyed steel (kg)	1,900
Plastic (kg)	300
Electronic material, power, control (kg)	1,100
Process material, adsorbent, lubricant (kg)	200
Concrete (kg)	5,600

Declaration of competing interest

The authors declare that they have no known competing financial interests or personal relationships that could have appeared to influence the work reported in this paper.

Acknowledgments

This research work was funded by the Engineering and Physical Science Research Council under the Zero-Carbon Emission Integrated Cooling, Heating and Power (ICHP) Networks (EP/T022949/1), A network for hydrogen-fuelled transportation (Network-H2) (EP/S032134/1), and United Kingdom CCS Research Centre (UKCCSRC) grant (EP/W002841/1).

Appendix

Data availability

Our research data are published in the Durham University Research Data Repository. DOI: http://doi.org/10.15128/r2v118rd59q

References

[1] GOI. Annual Report. 2022.
[2] GOI. Distribution Schemes 2023. https://powermin.gov.in/en/content/overview-1#:~:text="The erstwhile Rajiv Gandhi Grameen,Agency for implementation of DDUGJY.
[3] Das S, De S. Technically efficient, economic and environmentally benign hybrid decentralized energy solution for an Indian village: Multi criteria decision making approach. J Clean Prod 2023;388:135717. https://doi.org/10.1016/j.jclepro.2022.135717.
[4] Hasan GMJ, Jabir A Al, Anam MM. Monitoring bank-line movements of the rivers flowing across the Sundarbans using remote sensing and GIS techniques. Reg Stud Mar Sci 2022;56:102679. DOI: 10.1016/j.rsma.2022.102679.
[5] Paul T. Need assessment and detailed planning for a harmonious hydrometeorology system for the Sundarbans (Vol. 2) : Looking at Comparable Deltas : Experiences from Mekong (Inglês). 2019.
[6] Mansouri SA, Ahmarinejad A, Nematbakhsh E, Javadi MS, Esmaeel Nezhad A, Catalão JPS. A sustainable framework for multi-microgrids energy management in automated distribution network by considering smart homes and high penetration of renewable energy resources. Energy 2022;245. https://doi.org/10.1016/j.energy.2022.123228.
[7] Wwf. Community Solar Micro Grid Provide a Ray of Hope in Sundarbans in aftermath of cyclone Amphan. World Wide Fund Nature-India 2023. https://www.wwfindia.org/news_facts/feature_stories/community_solar_micro_grids_provide_a_ray_of_hope/.
[8] Ul Islam Z, Hossain Lipu MS, Karim TF, Fuad AM, Ali MMN, Shihavuddin ASM, et al. Optimizing hybrid renewable energy based automated railway level crossing in Bangladesh: Techno-economic, emission and sensitivity analysis. Energy Convers Manag X 2024;24. DOI: 10.1016/j.ecmx.2024.100744.
[9] Ul Rehman N, Farzaneh H. Techno-economic analysis of a hybrid heat recovery-renewable energy system for enhancing power reliability in cement factories in Pakistan. Energy Convers Manag X 2023;20:100492. https://doi.org/10.1016/j.ecmx.2023.100492.
[10] Sadeghi A, Maleki A, Haghighat S. Techno-Economic Analysis and Optimization of a Hybrid Solar-Wind- Biomass-Battery Framework for the Electrification of a Remote Area : A. Energy Convers Manag X 2024:100732. DOI: 10.1016/j.ecmx.2024.100732.
[11] Ashraful Islam M, Naushad Ali MM, Mollick T, Islam A, Benitez IB, Sidi Habib S, et al. Assessing the feasibility and quality performance of a renewable Energy-Based hybrid microgrid for electrification of remote communities. Energy Convers Manag X 2024;23:100674. https://doi.org/10.1016/j.ecmx.2024.100674.
[12] Singh U, Rizwan M. A feasibility study and cost benefit analysis of an off-grid hybrid system for a rural area electrification. Sol Compass 2022;3–4:100031. https://doi.org/10.1016/j.solcom.2022.100031.
[13] Xu X, Zhang Z, Yuan J, Shao J. Design and multi-objective comprehensive evaluation analysis of PV-WT-BG-Battery hybrid renewable energy systems in urban communities. Energy Convers Manag X 2023;18:100357. https://doi.org/10.1016/j.ecmx.2023.100357.
[14] Kumar R, Channi HK. A PV-Biomass off-grid hybrid renewable energy system (HRES) for rural electrification: Design, optimization and techno-economic-environmental analysis. J Clean Prod 2022;349:131347. https://doi.org/10.1016/j.jclepro.2022.131347.
[15] Ngila A, Farzaneh H. Energy Conversion and Management : X Techno-economic analysis and dynamic power simulation of a hybrid solar-wind-battery-flywheel system for off-grid power supply in remote areas in Kenya Introduction : Energy Convers Manag X 2023;18:100381. DOI: 10.1016/j.ecmx.2023.100381.
[16] He Y, Guo S, Dong P, Huang J, Zhou J. Hierarchical optimization of policy and design for standalone hybrid power systems considering lifecycle carbon reduction subsidy. Energy 2023;262. https://doi.org/10.1016/j.energy.2022.125454.
[17] El-houari H, Allouhi A, Rehman S, Buker MS, Kousksou T, Jamil A, et al. Feasibility evaluation of a hybrid renewable power generation system for sustainable electricity supply in a Moroccan remote site. J Clean Prod 2020;277:123534. https://doi.org/10.1016/j.jclepro.2020.123534.
[18] Roy D. Modelling an off-grid hybrid renewable energy system to deliver electricity to a remote Indian island. Energy Convers Manag 2023;281:116839. https://doi.org/10.1016/j.enconman.2023.116839.
[19] Ashraful Islam M, Naushad Ali MM, Al Mamun A, Shahadat Hossain M, Hasan Maruf M, Shihavuddin ASM. Optimizing energy solutions: A techno-economic analysis of solar-wind hybrid power generation in the coastal regions of Bangladesh. Energy Convers Manag X 2024;22:100605. https://doi.org/10.1016/j.ecmx.2024.100605.
[20] Das S, Pradhan S, De S. Multi criteria decision making for the most suitable combination of energy resources for a decentralized hybrid energy solution with green hydrogen as the storage option. Energy Convers Manag 2023;285:117028. https://doi.org/10.1016/j.enconman.2023.117028.
[21] Das S, Ray A, De S. Comparative analysis of storage modules under different dispatch strategies for an optimum decentralized hybrid energy solution: a case study of a remote Indian village. Clean Technol Environ Policy 2022;24:2495–515. https://doi.org/10.1007/s10098-022-02330-0.
[22] Peppas A, Kollias K, Politis A, Karalis L, Taxiarchou M, Paspaliaris I. Performance evaluation and life cycle analysis of RES-hydrogen hybrid energy system for office building. Int J Hydrogen Energy 2021;46:6286–98. https://doi.org/10.1016/j.ijhydene.2020.11.173.
[23] Khan FI, Hawboldt K, Iqbal MT. Life Cycle Analysis of wind-fuel cell integrated system. Renew Energy 2005;30:157–77. https://doi.org/10.1016/j.renene.2004.05.009.

[24] Lai H, Adams TA. Life cycle analyses of SOFC/gas turbine hybrid power plants accounting for long-term degradation effects. J Clean Prod 2023;412:137411. https://doi.org/10.1016/j.jclepro.2023.137411.
[25] Rillo E, Gandiglio M, Lanzini A, Bobba S, Santarelli M, Blengini G. Life Cycle Assessment (LCA) of biogas-fed Solid Oxide Fuel Cell (SOFC) plant. Energy 2017;126:585–602. https://doi.org/10.1016/j.energy.2017.03.041.
[26] Jolaoso LA, Duan C, Kazempoor P. Life cycle analysis of a hydrogen production system based on solid oxide electrolysis cells integrated with different energy and wastewater sources. Int J Hydrogen Energy 2023. https://doi.org/10.1016/j.ijhydene.2023.07.129.
[27] Nagapurkar P, Smith JD. Techno-economic optimization and environmental Life Cycle Assessment (LCA) of microgrids located in the US using genetic algorithm. Energy Convers Manag 2019;181:272–91. https://doi.org/10.1016/j.enconman.2018.11.072.
[28] Aberilla JM, Gallego-Schmid A, Stamford L, Azapagic A. Design and environmental sustainability assessment of small-scale off-grid energy systems for remote rural communities. Appl Energy 2020;258:114004. https://doi.org/10.1016/j.apenergy.2019.114004.
[29] Mayer MJ, Szilágyi A, Gróf G. Environmental and economic multi-objective optimization of a household level hybrid renewable energy system by genetic algorithm. Appl Energy 2020;269:115058. https://doi.org/10.1016/j.apenergy.2020.115058.
[30] Memon SA, Upadhyay DS, Patel RN. Optimal configuration of solar and wind-based hybrid renewable energy system with and without energy storage including environmental and social criteria: A case study. J Energy Storage 2021;44:103446. https://doi.org/10.1016/j.est.2021.103446.
[31] Gonzalez A, Riba JR, Esteban B, Rius A. Environmental and cost optimal design of a biomass–Wind–PV electricity generation system. Renew Energy 2018;126:420–30. https://doi.org/10.1016/j.renene.2018.03.062.
[32] Kiehbadroudinezhad M, Merabet A, Hosseinzadeh-Bandbafha H, Ghenai C. Environmental assessment of optimized renewable energy-based microgrids integrated desalination plant: considering human health, ecosystem quality, climate change, and resources. Environ Sci Pollut Res 2023;30:29888–908. https://doi.org/10.1007/s11356-022-24051-z.
[33] Roy D, Bhowmik M, Roskilly AP. Technoeconomic, environmental and multi criteria decision making investigations for optimisation of off-grid hybrid renewable energy system with green hydrogen production. J Clean Prod 2024;443:141033. https://doi.org/10.1016/j.jclepro.2024.141033.
[34] Ifaei P, Yoo CK. The compatibility of controlled power plants with self-sustainable models using a hybrid input/output and water-energy-carbon nexus analysis for climate change adaptation. J Clean Prod 2019;208:753–77. https://doi.org/10.1016/j.jclepro.2018.10.150.
[35] El Hassani S, Oueslati F, Horma O, Santana D, Moussaoui MA, Mezrhab A. Techno-economic feasibility and performance analysis of an islanded hybrid renewable energy system with hydrogen storage in Morocco. J Energy Storage 2023;68:107853. https://doi.org/10.1016/j.est.2023.107853.
[36] Krishan O, Suhag S. Techno-economic analysis of a hybrid renewable energy system for an energy poor rural community. J Energy Storage 2019;23:305–19. https://doi.org/10.1016/j.est.2019.04.002.
[37] Esfilar R, Bagheri M, Golestani B. Technoeconomic feasibility review of hybrid waste to energy system in the campus: A case study for the University of Victoria. Renew Sustain Energy Rev 2021;146:111190. https://doi.org/10.1016/j.rser.2021.111190.
[38] Kushwaha PK, Ray P, Bhattacharjee C. Optimal Sizing of a Hybrid Renewable Energy System: A Socio-Techno-Economic-Environmental Perspective. J Sol Energy Eng 2022;145. https://doi.org/10.1115/1.4055196.
[39] Das BK, Hassan R, Tushar MSHK, Zaman F, Hasan M, Das P. Techno-economic and environmental assessment of a hybrid renewable energy system using multi-objective genetic algorithm: A case study for remote Island in Bangladesh. Energy Convers Manag 2021;230:113823. https://doi.org/10.1016/j.enconman.2020.113823.
[40] Kharrich M, Selim A, Kamel S, Kim J. An effective design of hybrid renewable energy system using an improved Archimedes Optimization Algorithm: A case study of Farafra. Egypt Energy Convers Manag 2023;283:116907. https://doi.org/10.1016/j.enconman.2023.116907.
[41] Memon SA, Upadhyay DS, Patel RN. Optimization of solar and battery-based hybrid renewable energy system augmented with bioenergy and hydro energy-based dispatchable source. Iscience 2023;26:105821. https://doi.org/10.1016/j.isci.2022.105821.
[42] United Nations. Ensure access to affordable, reliable, sustainable and modern energy for all. United Nations 2022. https://sdgs.un.org/goals/goal7.
[43] Thakur S, Hazra S, Ghosh T. Biomass Burning and Natural Vegetation Loss as a Consequence to Government Policy : A Case Study of Satjelia Island. Indian Sundarban Delta 2019. https://doi.org/10.1729/Journal.20025.
[44] Das P, Das BK, Rahman M, Hassan R. Evaluating the prospect of utilizing excess energy and creating employments from a hybrid energy system meeting electricity and freshwater demands using multi-objective evolutionary algorithms. Energy 2022;238. https://doi.org/10.1016/j.energy.2021.121860.
[45] Khan FA, Pal N, Saeed SH. Optimization and sizing of SPV/Wind hybrid renewable energy system: A techno-economic and social perspective. Energy 2021;233:121114. https://doi.org/10.1016/j.energy.2021.121114.
[46] NASA. The POWER Project 2024. https://power.larc.nasa.gov/.
[47] MNRE. National Green Hydrogen Mission 2024. https://mnre.gov.in/national-green-hydrogen-mission/#:~:text=The National Green Hydrogen Mission, efficiently transport and distribute hydrogen.
[48] Mousavi SA, Zarchi RA, Astaraei FR, Ghasempour R, Khaninezhad FM. Decision-making between renewable energy configurations and grid extension to simultaneously supply electrical power and fresh water in remote villages for five different climate zones. J Clean Prod 2021;279:123617. https://doi.org/10.1016/j.jclepro.2020.123617.
[49] Alsagri AS, Alrobaian AA, Nejlaoui M. Techno-economic evaluation of an off-grid health clinic considering the current and future energy challenges: A rural case study. Renew Energy 2021;169:34–52. https://doi.org/10.1016/j.renene.2021.01.017.
[50] Rad MAV, Ghasempour R, Rahdan P, Mousavi S, Arastounia M. Techno-economic analysis of a hybrid power system based on the cost-effective hydrogen production method for rural electrification, a case study in Iran. Energy 2020;190:116421. https://doi.org/10.1016/j.energy.2019.116421.
[51] Elmorshedy MF, Elkadeem MR, Kotb KM, Taha IBM, Mazzeo D. Optimal design and energy management of an isolated fully renewable energy system integrating batteries and supercapacitors. Energy Convers Manag 2021;245:114584. https://doi.org/10.1016/j.enconman.2021.114584.
[52] Razmjoo A, Gakenia Kaigutha L, Vaziri Rad MA, Marzband M, Davarpanah A, Denai M. A Technical analysis investigating energy sustainability utilizing reliable renewable energy sources to reduce CO2 emissions in a high potential area. Renew Energy 2021;164:46–57. https://doi.org/10.1016/j.renene.2020.09.042.
[53] Iso. Environmental Management-lige cycle assessment-principles and framework. Int Organ Stand 2006. https://www.iso.org/standard/37456.html.
[54] Iso. Environmental management — Life cycle assessment — Requirements and guidelines. Int Organ Stand 2006. https://www.iso.org/standard/38498.html.
[55] Greening B, Azapagic A. Environmental impacts of micro-wind turbines and their potential tocontribute to UK climate change targets. Energy 2013;59:454–66. https://doi.org/10.1016/j.energy.2013.06.037.
[56] ecoinvent. Ecoinvent 3.9.1. 2022.
[57] Bareiß K, de la Rua C, Möckl M, Hamacher T. Life cycle assessment of hydrogen from proton exchange membrane water electrolysis in future energy systems. Appl Energy 2019;237:862–72. https://doi.org/10.1016/j.apenergy.2019.01.001.
[58] Yadav S, Kumar P, Kumar A. Techno-economic assessment of hybrid renewable energy system with multi energy storage system using HOMER. Energy 2024;297:131231. https://doi.org/10.1016/j.energy.2024.131231.
[59] Baghel N, Manjunath K, Kumar A. Assessment of Solar-Biomass Hybrid Power System for Decarbonizing and Sustainable Energy Transition for Academic Building. Process Saf Environ Prot 2024;187:1201–12. https://doi.org/10.1016/j.psep.2024.05.004.
[60] Ahmed MM, Das BK, Das P, Hossain MS, Kibria MG. Energy management and sizing of a stand-alone hybrid renewable energy system for community electricity, fresh water, and cooking gas demands of a remote island. Energy Convers Manag 2024;299:117865. https://doi.org/10.1016/j.enconman.2023.117865.
[61] Das P, Das BK, Islam MS, Rahman M, Hassan R, Shuvo KA. Investigation of a reliable and sustainable stand-alone hybrid energy system for freshwater supply: a case study. Int J Sustain Energy 2023;42:236–67. https://doi.org/10.1080/14786451.2023.2185866.
[62] Afonaa-Mensah S, Odoi-Yorke F, Babatunde MI. Evaluating the impact of industrial loads on the performance of solar PV/diesel hybrid renewable energy systems for rural electrification in Ghana. Energy Convers Manag X 2024;21:100525. https://doi.org/10.1016/j.ecmx.2024.100525.
[63] Ahmad R, Farzaneh H. Techno-economic analysis and dynamic power simulation of a hybrid solar-wind-battery system for power supply in rural areas in Pakistan. Clean Energy Syst 2024;100127. https://doi.org/10.1016/j.ecmx.2023.100381.
[64] Williams L, Wang Y. A distributed renewable power system with hydrogen generation and storage for an island. Appl Energy 2024;358:122500. https://doi.org/10.1016/j.apenergy.2023.122500.
[65] Allouhi A. A hybrid PV/wind/battery energy system to assist a run-of-river micro-hydropower for clean electrification and fuelling hydrogen mobility for young population in a rural Moroccan site. J Clean Prod 2024;442:140852. https://doi.org/10.1016/j.jclepro.2024.140852.
[66] Kolhe ML, Ranaweera KMIU, Gunawardana AGBS. Techno-economic sizing of off-grid hybrid renewable energy system for rural electrification in Sri Lanka. Sustain Energy Technol Assessments 2015;11:53–64. https://doi.org/10.1016/j.seta.2015.03.008.
[67] Khan T, Waseem M, Tahir M, Liu S, Yu M. Autonomous hydrogen-based solar-powered energy system for rural electrification in Balochistan, Pakistan: An energy-economic feasibility analysis. Energy Convers Manag 2022;271:116284. https://doi.org/10.1016/j.enconman.2022.116284.
[68] Mojumder MFH, Islam T, Chowdhury P, Hasan M, Takia NA, Chowdhury NUR, et al. Techno-economic and environmental analysis of hybrid energy systems for remote areas: A sustainable case study in Bangladesh. Energy Convers Manag X 2024;23:100664. https://doi.org/10.1016/j.ecmx.2024.100664.
[69] Dost Mohammadi SA, Gezegin C. Feasibility investigation and economic analysis of photovoltaic, wind and biomass hybrid systems for rural electrification in Afghanistan. Electr Eng 2024;106:2821–41. https://doi.org/10.1007/s00202-023-02115-8.
[70] Khare V, Khare CJ, Bhuiyan MA. Design, optimization, and data analysis of solar-tidal hybrid renewable energy system for Hurawalhi. Maldives Clean Energy Syst 2023;6:100088. https://doi.org/10.1016/j.cles.2023.100088.
[71] Neupane D, Kafle S, Gurung S, Neupane S, Bhattarai N. Optimal sizing and financial analysis of a stand-alone SPV-micro-hydropower hybrid system considering generation uncertainty. Int J Low-Carbon Technol 2021;16:1479–91. https://doi.org/10.1093/ijlct/ctab077.
[72] XE. XE.com Inc (https://www.xe.com/) 2024.
[73] PIB. Net zero emissions target. 2023.

[74] Khan FA, Pal N, Saeed SH, Yadav A. Modelling and techno-economic analysis of standalone SPV/Wind hybrid renewable energy system with lead-acid battery technology for rural applications. J Energy Storage 2022;55:105742. https://doi.org/10.1016/j.est.2022.105742.

[75] Akhtari MR, Shayegh I, Karimi N. Techno-economic assessment and optimization of a hybrid renewable earth - air heat exchanger coupled with electric boiler, hydrogen, wind and PV configurations. Renew Energy 2020;148:839–51. https://doi.org/10.1016/j.renene.2019.10.169.

[76] Li J, Liu P, Li Z. Optimal design and techno-economic analysis of a hybrid renewable energy system for off-grid power supply and hydrogen production: A case study of West China. Chem Eng Res Des 2022;177:604–14. https://doi.org/10.1016/j.cherd.2021.11.014.

[77] Hossein Jahangir M, Bazdar E, Kargarzadeh A. Techno-economic and environmental assessment of low carbon hybrid renewable electric systems for urban energy planning: Tehran-Iran. City Environ Interact 2022;16:100085. https://doi.org/10.1016/j.cacint.2022.100085.